Improvements in BSCF CATHODES for low temperature solid oxide fuel cells

P. V. C. K. Subhashini[1]*

[1] Research Scholar, Department of Mechanical Engineering,

Department of Technical Education, Telangana State, India

* Corresponding author e-mail: subha.pvck@gmail.in

Phone +91 9849672858

Abstract

In the present work, Cathode powders were synthesized through a solid-state reaction process. The primary aim was to reduce the coefficient of thermal expansion (CTE) by decreasing the cobalt content and introducing magnesium doping, targeting application in low-temperature solid oxide fuel cells (SOFCs). Measurements of relative density indicated the presence of porosity in the fabricated cathodes. A noticeable improvement in densification was observed as the sintering temperature increased from 900 °C to 1175 °C. X-ray diffraction (XRD) analysis performed on all compositions confirmed the retention of a single-phase perovskite structure, with no additional phases detected. The average crystallite size was determined to be approximately 18 nm. The cathodes were fabricated in two configurations: layered composites and mixed composites. Their electrochemical behavior was evaluated using electrochemical impedance spectroscopy (EIS) at an intermediate operating temperature of 700 °C under ambient air conditions. Cathode films were deposited on the electrolyte surface and sintered at three different temperatures 900 °C, 950 °C, and 1000 °C to examine the influence of sintering temperature on cell performance. Among these, the cell sintered at 900 °C exhibited the lowest polarization

resistance, indicating superior electrochemical activity. Notably, the nano-composite cathodes demonstrated reduced values compared to traditional LSMO cathodes. Specifically, the polarization resistance was measured as 2.72 Ω·cm² for the layered structure and 1.76 Ω·cm² for the mixed composite design. These findings highlight the promise of using LSMO-BSCMF composites particularly in a mixed configuration as cathode materials for low-temperature SOFCs, offering enhanced performance through reduced polarization losses

Keywords: SOFC, BSCF, cathode, polarization resistance, magnesium, polarization potential.

1. Introduction

In recent times, research into clean energy technologies based on fuel cells has drawn considerable interest, largely due to the environmental challenges and limitations posed by fossil fuels. Fuel cells generate electricity through the direct conversion of chemical energy, producing minimal emissions compared to conventional fossil fuel-based systems [1]. Among the different types of fuel cells, solid oxide fuel cells (SOFCs) are regarded as particularly promising due to their fuel flexibility, cost-effective electrode materials, moderate operating temperatures, and relatively straightforward operational requirements [2]. Operating SOFCs at lower temperatures offers additional advantages, such as simplified system design and reduced thermal stress on components [3]. However, a key drawback is that the performance and efficiency of SOFCs tend to decline as the operating temperature decreases [4]. To overcome this challenge, recent advancements in ion-doped cathode materials have shown significant potential in improving fuel cell performance, especially under low-temperature conditions [4]. In recent years, extensive research has focused on the development of low-temperature solid oxide fuel cells (SOFCs) to minimize the challenges associated with high-temperature operation [5]. However, reducing the

operating temperature often leads to a decline in overall cell efficiency [6, 7]. Another critical concern at lower temperatures is the increased polarization loss at the cathode–electrolyte interface, which adversely affects electrochemical performance. One effective approach to overcoming these limitations is through ion doping of cathode materials, which has shown promising results in enhancing cell output under reduced-temperature conditions. By modifying the chemical composition of the cathode, it is possible to boost oxygen surface exchange kinetics while maintaining a stable coefficient of thermal expansion (CTE) [8]. Perovskite-structured materials with the general formula ABO_3 are commonly selected as cathode materials for solid oxide fuel cells (SOFCs), where the A and B sites are occupied by different cations [9-11]. These materials have been widely studied for their electrochemical properties, and among them, the $Ba_{0.5}Sr_{0.5}Co_{0.8}Fe_{0.2}O_{3-\delta}$ (BSCF) system has shown considerable potential according to several studies [12–16]. However, a major limitation of BSCF is its high cobalt (Co) content, which leads to an elevated coefficient of thermal expansion (CTE)—a drawback for long-term stability and compatibility with other cell components [17]. To overcome this issue, researchers have explored doping strategies to substitute appropriate ions into the BSCF structure, thereby enhancing cell performance without compromising material stability [18, 19]. For instance, Liu et al. [20] reported enhanced oxygen reduction reaction (ORR) activity by introducing Ce, La, and Pr at the B-site of the BSCF lattice. Similarly, Zeng et al. [21] demonstrated that Zn doping improved the electrocatalytic activity of BSCF, attributed to favorable modifications in the material's surface chemistry. Other studies have reported positive effects from doping with Mo^{6+}, Nb^{3+}, and Y^{3+} ions, all contributing to improved SOFC performance [22–25]. Despite these advancements, limited research has been conducted on the effect of Mg doping in BSCF cathode materials. Therefore, the present study aims to develop a SOFC using Mg-doped BSCF

as the cathode material and Gadolinium-doped Ceria (GDC) as the electrolyte, with a focus on evaluating the electrochemical performance of the resulting cell [26, 27].

2. Experimental details

The specific synthesis procedure and exact quantities used to prepare the cathode material are available in our previous publication [28]. Among the various compositions studied within the BSCMF system, the formulation $Ba_{0.5}Sr_{0.5}(Co_{0.2}Mg_{0.8})_{0.2}Fe_{0.8}O_3$ was found to deliver superior performance compared to other Co-Mg ratios [29]. Lanthanum strontium manganite oxide (LSMO) nanopowder, with a particle size range of 50–100 nm, was sourced from Sigma-Aldrich (India) and blended with the BSCMF powder to fabricate a nanocomposite cathode. An equal weight ratio (50 wt%) of each powder was used to produce the composite material[30]. The powders were thoroughly mixed using ball milling, followed by calcination and sieving to eliminate larger particles. Two types of composite cathodes were then fabricated based on this blend. For the first configuration, a layered composite cathode was created by depositing an LSMO layer on top of the Mg-doped BSCMF layer. Gadolinium-doped ceria (GDC) powder, with an average particle size of 40 nm, was obtained from Advanced Materials, India, and used as the electrolyte material for cell fabrication[31]. To prepare the cathode inks, BSCMF powders of the desired composition were mixed with terpineol as the solvent and ethyl cellulose as the binder. The resulting mixture was subjected to magnetic stirring for 4 hours to ensure homogeneity. The prepared inks were then screen-printed onto both sides of circular GDC electrolyte pellets, each 10 mm in diameter. The BSCMF ink was applied uniformly over the entire 10 mm surface area on both sides of the electrolyte [32]. After printing, the samples were dried and sintered at 1100 °C for 2 hours to promote good adhesion and to develop the desired

porosity in the BSCMF thin film cathode layers. The final thickness of the cathode films was approximately 2–3 μm. This configuration is known as a symmetric cell, where identical cathode materials are applied on both sides of the electrolyte. For current collection, silver ink was screen-printed on top of the cathode layers on both sides and then cured to ensure firm contact and reliable conductivity. The impact of magnesium (Mg) doping levels in the BSCF system on cathode performance was evaluated using electrochemical impedance spectroscopy (EIS) under this symmetric cell setup.

3. Results and discussion

Figure 1 displays the X-ray diffraction (XRD) patterns of the BSCF-based cathode powders. ll diffraction peaks were indexed using JCPDS card No. 55-0563, confirming the formation of a cubic perovskite oxide structure with space group $Pm\bar{3}m$**.** No noticeable peaks corresponding to secondary phases or impurities were detected, indicating high phase purity of the synthesized powders. A slight shift in the (110) diffraction peak was observed, which is attributed to the increasing magnesium (Mg) substitution at the cobalt (Co) sites on the B-site of the perovskite lattice. This substitution leads to a variation in the lattice parameter, which in turn causes a shift in the high-intensity peaks typically associated with the cubic BSCF phase. The overall diffraction pattern is in good agreement with the standard JCPDS data and aligns well with previously reported literature [13].

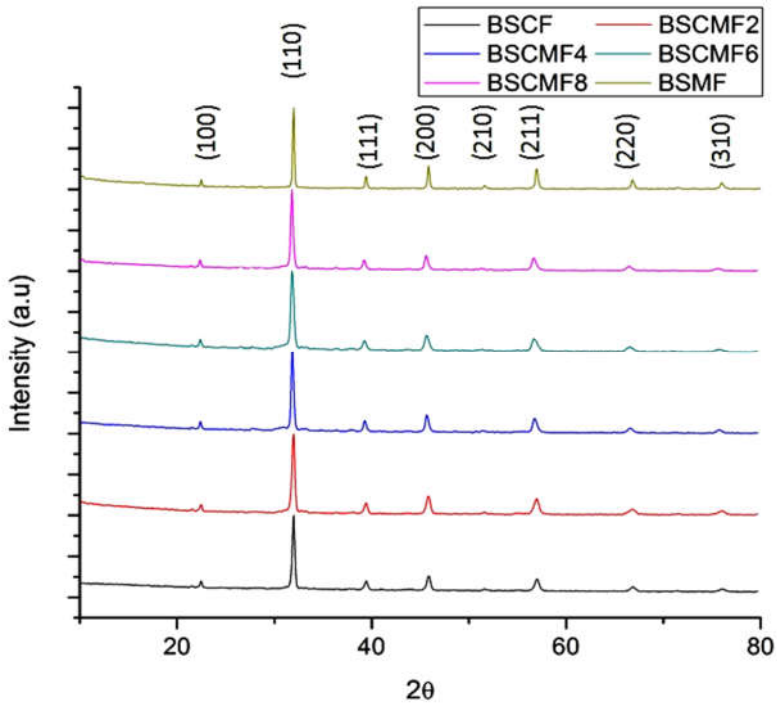

Fig 1 XRD patterns of the BSCF cathode materials

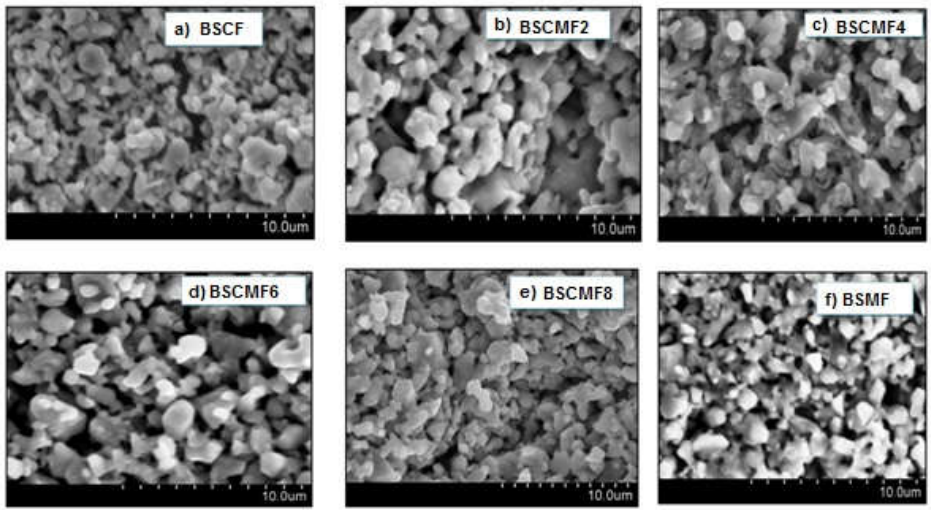

Fig 2 SEM images showing the morphologies of the BSCF cathode materials

Figure 2 presents the micrographs of BSCF cathode films sintered at 900 °C for 2 hours, prepared for symmetric cell configuration. The microstructural analysis reveals a well-developed

porous network with grains exhibiting good necking, indicative of effective sintering. Across all cathode compositions studied, no major variation in grain morphology was detected. However, an increase in porosity was clearly observed with higher levels of magnesium (Mg) substitution. This enhanced porosity, resulting from Mg incorporation at the B-site, contributes to a greater number of triple phase boundaries (TPBs) within the cathode layer. An increased TPB density is beneficial for improving oxygen reduction kinetics and facilitates better gas diffusion through the porous structure. Furthermore, the presence of finer particles in the initial cathode powders also plays a crucial role in promoting TPB formation, ultimately leading to improved electrochemical performance when compared to other compositions

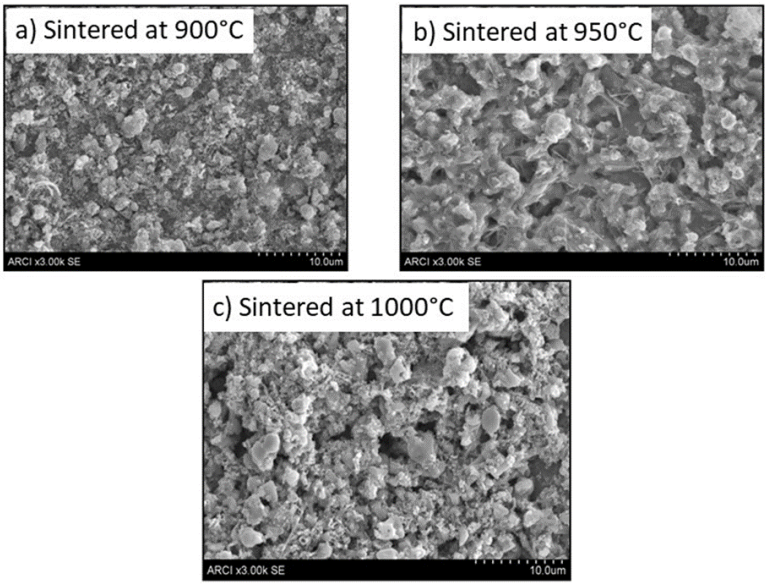

Fig. 3. SEM micrographs of sintered mixed composite cathodes sintered at: (a) 900℃, (b) 950℃ and (c) 1000℃.

Figure 3 shows the microstructural images of the mixed composite cathode films sintered at three different temperatures: 900 °C, 950 °C, and 1000 °C. As the sintering temperature increases, localized segregation within the cathode layer becomes evident in certain regions. This segregation indicates the possible formation of resistive phases at the cathode–electrolyte interface at higher sintering temperatures, which could lead to an increase in ohmic resistance. To further investigate the impact of sintering temperature presents the impedance spectra of the symmetric cells using the mixed composite cathode, measured at 700 °C. The observed semicircular arcs in the Nyquist plot correspond to different electrochemical processes occurring over specific frequency ranges. With increasing sintering temperature, a noticeable rise in polarization resistance (R) is observed across the entire frequency spectrum. This trend suggests a decline in porosity and a corresponding reduction in the number of active triple phase boundaries (TPBs), which are critical for efficient gas diffusion and electrochemical activity.

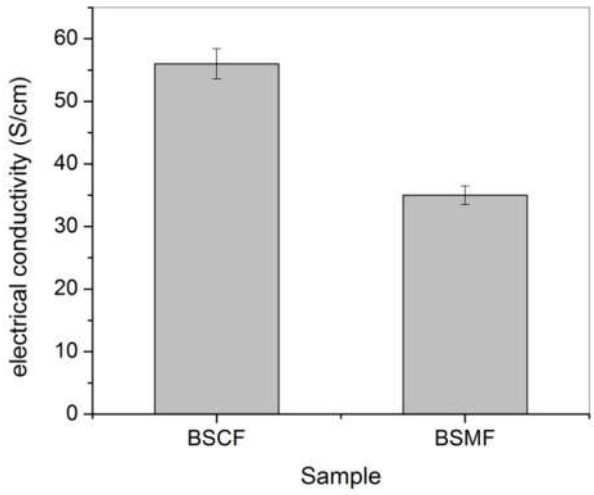

Fig 4 Electric conductivity of the BSCF and BSMF cathode materials

Figure 4 illustrates the electrical conductivity (σ) of the cathode materials, as measured by the DC four-probe technique. The results show that the BSMF cathode exhibits a lower conductivity of 35 ± 1.6 S/cm**,** in comparison to the BSCF cathode, which recorded a higher value of 56 ± 2.4 S/cm**.** This clearly demonstrates that magnesium (Mg) doping leads to a noticeable reduction in electrical conductivity when compared to the cobalt-rich BSCF composition. The lower conductivity in the BSMF sample can be attributed to the greater chemical stability of Mg^{2+} ions relative to Co ions. Although both BSCF and BSMF cathodes function as mixed ionic and electronic conductors, the electronic contribution is diminished in the Mg-doped variant due to the reduced availability of Co ions, which are primarily responsible for electron transport.

4. Conclusions

$Ba_{0.5}Sr_{0.5}(Co_{1-x}Mg_x)_{0.2}Fe_{0.8}O_3$ (x=0, 0.2, 0.4, 0.6, 0.8, 1) cathode materials have been produced and the effect of magnesium (Mg) doping on cathode performance has been evaluated. The produced cathodes were used to prepare symmetric cell configuration with gadolinium doped cerium (GDC) as the electrolyte. XRD analysis confirms the cubic perovskite structure in the cathode materials. The porosity has been observed as increased with the increased content of Mg as confirmed from the SEM images. From the electrochemical impedance spectroscopy (EIS) studies, of the cathode symmetric cells measured from 600ºC to 700ºC under open circuit state, the polarization resistance (R_P) values were recorded. At 7000 °C, the polarization resistance of BSCF is 13.96 ohm-cm^2 and with the addition of Mg it has decreased to 5.17 ohm-cm^2. Further increase in the Mg concentration decreased the polarization resistance up to 0.34 ohm-cm2, which is the minimum value obtained in the composition BSCMF8. Higher charge transfer (CT) was observed in the case of Mg-rich compositions, representing the presence of Mg that can improve the oxygen permeation flux. On the other hand, higher oxygen reduction reaction

(ORR) was observed in the case of Co rich compositions, representing Co that can enhance the oxygen vacancy concentration that is responsible for the oxygen ionic conductivity. It is clear from the results that with the increase of temperature, R_P value decreases. With the increase of magnesium concentration in the cathode, R_P value is observed as decreased. This is due to the high oxygen permeation flux behavior of magnesium, which is in the B-site of the cathode. From the results, BSCMF (with $Mg_{0.8}$ and $Co_{0.2}$) has been observed with lower polarization resistance compared with the other compositions, deciding the optimum concentration of magnesium and cobalt to be present in the B-site of the cathode. The thermal expansion coefficient of BSCMF8 (17.45×10^{-6}/K) was measured as lower compared with BSCF (22.1×10^{-6}/K) due to the constant oxidation state of Mg which suppressed the chemical expansion caused by Co ions. Hence, for the present work, it can be concluded that BSCF cathode system with $Mg_{0.8}$ and $Co_{0.2}$ compositionis the optimum to yield better performance in the low temperature SOFCs.

References

1. Lixin Fan, Zhengkai Tu, Siew Hw Chan, *Energy Rep***7** (2021) 8421-8446.
2. SinghalS C, Kendal K, *High Temperature Solid Oxide Fuel Cells*, Elsevier, Netherlands 2003.
3. Qidong Xu, Zengjia Guo, Lingchao Xia, Qijiao He, Zheng Li, Idris Temitope Bello, Keqing Zheng, Meng Ni, *Energy Convers. Manag.* **253** (2022) 115175
4. Lee K T, WachsmanE D, *MRS Bull* **39** (2014) 783.
5. Chen Y, Zhou W, Ding D, Liu M, Ciucci F, Tade M, Shao Z, *Adv Energy Mater* **5** (2015) 1500537
6. Dai H, Kou H, Tao Z, Liu K, Xue M, Zhang Q, Bi L, *Ceram Int* **46** (2020) 6987.
7. Choi S, Yoo S, Kim J, Park S, Jun A, Sengodan S, Kim J, Shin J, Jeong H Y, Choi Y, Kim G, Liu M, *Sci Rep* **3** (2013) 3.
8. Chen Y, Zhou W, Ding D, Liu M, Ciucci F, Tade M, Shao Z, *Adv Energy Mater* **5** (2015) 1500537

9. Dai H, Kou H, Tao Z, Liu K, Xue M, Zhang Q, Bi L, *Ceram Int* **46** (2020) 6987.
10. Choi S, Yoo S, Kim J, Park S, Jun A, Sengodan S, Kim J, Shin J, Jeong H Y, Choi Y, Kim G, Liu M, *Sci Rep* **3** (2013) 3.
11. Wang B, Bi L, Zhao X S, *Ceram Int* **44** (2018) 5139.
12. Baumann FS, Fleig J, Cristiani G, Stuhlhofer B, Habermeier H U, Maier J, *JElectrochem Soc* **154**, (2007) B931.
13. Yusof U A, Rahman H A, *J Phys Conf Ser***1082** (2018) 012029.
14. Zheng J, Wang X, Yu J, Tian N, *Mater Res Express*, **8** (2021) 035502.
15. Dey S, Das S, Chaudhary S, Parvatalu D, Mukhopadhyay M, Paul S, Sharma A D, Mukhopadhyay J, *Scripta Mater***229** (2023) 115380.
16. Rafaqat M, Ali G, Ahmad N, Hassan S, Jafri M, Atiq S, Abbas G, Mustafa G M, Raza R, J Alloys compd**937** (2023) 168214.
17. Liu, D, Dou Y, Xia T, Li Q, Sun L, Huo L, Zhao H, *J Power Sources*, **494** (2021) 229778.
18. Zeng Q, Zhang X, Wang W, Zhang D, Jiang Y, Zhou X, Lin B, *Catalysts***10(2)** (2020) 235.
19. Gou M, Ren R, Sun W, Xu C, Meng X, Wang Z, Qiao J, Sun K, *Ceram Int***45(12)** (2019) 15696 -15704.
20. Li X, Liu Y, Liu W, Wang C, Xu X, Dai H, Wang X, Bi L, *Sustain Energ Fuels*, **5** (2021) 4261-4267.
21. Meffert M, Unger L S, Störmer H, Sigloch F, Wagner S F, Ivers-Tiffée E, Gerthsen D, *J Am Ceram Soc* **102** (2019) 4929–4942.
22. Rafaqat M, Ali G, Ahmad N, Hassan S, Jafri M, Atiq S, Abbas G, Mustafa G M, Raza R, J Alloys compd**937** (2023) 168214.
23. Liu, D, Dou Y, Xia T, Li Q, Sun L, Huo L, Zhao H, *J Power Sources*, **494** (2021) 229778.
24. Zeng Q, Zhang X, Wang W, Zhang D, Jiang Y, Zhou X, Lin B, *Catalysts***10(2)** (2020) 235.

25. Gou M, Ren R, Sun W, Xu C, Meng X, Wang Z, Qiao J, Sun K, *Ceram Int***45(12)** (2019) 15696 -15704.

26. Li X, Liu Y, Liu W, Wang C, Xu X, Dai H, Wang X, Bi L, *Sustain Energ Fuels*, **5** (2021) 4261-4267.

27. Meffert M, Unger L S, Störmer H, Sigloch F, Wagner S F, Ivers-Tiffée E, GerthsenD, *J Am Ceram Soc* **102** (2019) 4929–4942.

28. Kamila R, Kurniawan B, *IOP Conf Ser: Mater Sci Eng***496** (2019) 012019.

29. Bilgili O, *Acta Phys Pol A,* **136** (2019) 460-466.

30. Pingbo X, Weiping Z, Kuo Y, Long J, Weiwei Z, Shangda X, *J Alloys Compd*, **311(1)** (2000) 90-92.

31. Da Conceião L, Silva A M, Ribeiro N F P, Souza M M V M, *Mater Res Bull*, **46 (2)** (2011) 308-314.

32. Chilkamarri Sameera Devi, Prasad G, *Trans Ind Ceram Soc***77(2)** (2018) 67-72